

Published in final edited form as:

Neurotoxicol Teratol. 2010 ; 32(1): 16. doi:10.1016/j.ntt.2009.06.002.

Image Analysis of Ca²⁺ Signals as a Basis for Neurotoxicity Assays: Promises and Challenges

Rola Barhoumi, Yongchang Qian, Robert C. Burghardt, and Evelyn Tiffany-Castiglioni
Department of Veterinary Integrative Biosciences Texas A&M University College Station, TX
77843-4458

Abstract

Free intracellular calcium ([Ca²⁺]_i) controls a wide range of cellular functions such as contraction, neurotransmitter and hormone release, metabolism, cell division and differentiation. Cytosolic Ca²⁺ levels are abnormal in cells exposed to toxicants and understanding how these levels become altered may improve our ability to design high-throughput methods for the sensitive detection of cellular responses to a toxic exposure. Because Ca²⁺ is involved in multiple aspects of cellular function, its role in signaling is complex. It is therefore necessary to identify the individual pathways targeted during toxicant exposure in order to use them as a tool for predictive measurements of toxicity and as targets for prevention or reversal of injury. This review illustrates several methods available for analysis of Ca²⁺ responses in vitro and their applicability for understanding mechanisms of toxicity at the molecular and cellular levels. The review will also consider the usefulness of Ca²⁺ imaging for predicting a unique signature for classes of toxicants. Towards this end, two methodological approaches for assessment of Ca²⁺ responses to toxicants are examined: steady state measurements and complex spatial and/or temporal measurements. Each of the methods described and appropriately used results in reliable and reproducible measurements which may be applied in a high-throughput fashion to individualize in vitro assessment of cellular responses caused by toxicants.

Keywords

Ca²⁺ waves; Ca²⁺ oscillations; Ca²⁺ modeling; toxicity; toxin exposure

1. Introduction

Free intracellular Ca²⁺ ([Ca²⁺]_i) is a ubiquitous intracellular second messenger or signal transducer involved in the control of a wide range of cellular functions required for metabolism and survival. A stimulus-induced increase in [Ca²⁺]_i is necessary for events such as contraction, neurotransmitter and hormone release, cell division, differentiation, and cell death. The calcium ion is capable of these diverse actions because [Ca²⁺]_i is tightly regulated in time and space within a cell. Perturbations of intracellular Ca²⁺ homeostasis are a common feature of cellular injuries and toxic exposures that lead to cell dysfunction and cytotoxicity [53], [3], and [69].

© 2009 Elsevier Inc. All rights reserved.

Corresponding Author: Rola Barhoumi, PhD. Department of Veterinary Integrative Biosciences Texas A&M University College Station, TX 77843-4458 Tel: (979) 458-1149 Fax: (979) 847-8981 Email: rmounieimne@cvm.tamu.edu.

Publisher's Disclaimer: This is a PDF file of an unedited manuscript that has been accepted for publication. As a service to our customers we are providing this early version of the manuscript. The manuscript will undergo copyediting, typesetting, and review of the resulting proof before it is published in its final citable form. Please note that during the production process errors may be discovered which could affect the content, and all legal disclaimers that apply to the journal pertain.

Analysis of Ca^{2+} signaling in cultured neuronal and glial cells has been employed to determine some of the complex cellular changes induced by environmental and pharmacologic neurotoxicants [2], [5], [7] and [47]. Also, alteration of intracellular Ca^{2+} homeostasis has been an important common mechanisms for environmental pollutants such as pyrethroids and organophosphate pesticides [16]. However, the use of Ca^{2+} signaling measurements for high-throughput screening of potential neurotoxicants has not yet been broadly applied, as it requires a much more precise identification of individual Ca^{2+} pathways targeted by toxicants than is routinely available. If such pathways were better understood, changes in their activities could be used as a predictive measurement of toxicity or for development of novel strategies for prevention or reversal of injury [4], and [5].

The resting $[\text{Ca}^{2+}]_i$ level in the cytosol is tightly regulated in the range of 100 nM, whereas extracellular Ca^{2+} levels are in the millimolar range. Maintenance of this steep gradient as well as regulation of Ca^{2+} transients that control many cellular processes are derived from two separate ON and OFF mechanisms (Figure 1) which constitute the Ca^{2+} signaling “toolkit” [11] and [54]. The ON mechanisms that increase $[\text{Ca}^{2+}]_i$ depend upon Ca^{2+} entry through channels in the plasma membrane or Ca^{2+} release from intracellular stores in the endoplasmic reticulum (ER) through ryanodine receptors (RYRs) or inositol 1,4,5-trisphosphate receptors (InsP3Rs). The OFF mechanisms remove Ca^{2+} from the cytosol by use of pumps in the plasma membrane or ER membrane. Other mechanisms for regulating cytosolic Ca^{2+} include cytosolic Ca^{2+} buffers and sequestration of Ca^{2+} in other organelles, such as mitochondria. Many chemicals and drugs are capable of affecting these ON and OFF mechanisms because each cell type has its own sensory mechanisms that can generate Ca^{2+} signals suitable to its physiology. Methods for analysis of the Ca^{2+} signal depend on the sensory mechanisms that generated it. In this report, screening methods are described for analysis of Ca^{2+} responses in astrocytes exposed to a variety of neurotoxicants. The utility of both steady state and dynamic Ca^{2+} responses are discussed relative to their potential for adaptation to high throughput screening of neurotoxicants.

2. Types of Ca^{2+} Signals

Increases in $[\text{Ca}^{2+}]_i$ that result from ON mechanisms are precisely encoded by their temporal and spatial organization. These Ca^{2+} signals act upon other signaling pathways in the cell which when activated can give rise to a variety of Ca^{2+} responses [50]. For example, localized puffs of Ca^{2+} occur with the opening of a small number of IP₃R Ca^{2+} channels within a cluster [55]. These “point source” of increased $[\text{Ca}^{2+}]_i$ are confined to a small region of the cytosol and are not propagated. In contrast, increases in $[\text{Ca}^{2+}]_i$ may occur as global transients (i.e., an integrated $[\text{Ca}^{2+}]_i$ response throughout the cell to a certain stimulus, irrespective of the origin or the starting point within the cell) or as spikes (i.e., a momentary sharp increase in $[\text{Ca}^{2+}]_i$ followed by a sharp decrease to the basal level). Transients can emanate from one point in a cell and propagate through the cell as waves. Waves are seen as a rise and fall of $[\text{Ca}^{2+}]_i$ that travels across the cell in milliseconds. Moreover, Ca^{2+} spikes or global transients can emanate from a cell and propagate through other cells as intercellular waves generated by mechanical or chemical stimuli if the cells are directly communicating either via gap junctions or paracrine signals (e.g., ATP).

In contrast to Ca^{2+} signals that are characterized by their amplitude, intracellular Ca^{2+} waves may also be propagated repetitively in the form of $[\text{Ca}^{2+}]_i$ oscillations of uniform frequency (reviewed in [8]). If waves are repetitive with a constant frequency within a cell, they are termed oscillations. In a few cell types such as astrocytes in culture, $[\text{Ca}^{2+}]_i$ oscillations may be intrinsically generated ([61]; personal observations); however, in most cells they are stimulated by specific receptor-activated chemicals. Their periodicity may range from seconds to many minutes and even hours. These oscillations are thought to constitute a frequency-

encoded signal with a high signal-to-noise ratio that limits prolonged exposure of cells to high $[Ca^{2+}]_i$ [64]. It is noteworthy that frequency- but not amplitude-encoded Ca^{2+} signals are efficiently transmitted into the mitochondria as a mitochondrial Ca^{2+} transient that activate mitochondrial dehydrogenases for ATP generation [28]. Mitochondria can therefore function to decode Ca^{2+} oscillations as well as transiently buffer cytosolic Ca^{2+} . The measurement of periodicity of cytosolic and mitochondrial Ca^{2+} oscillations by fluorescence imaging techniques in live cells is limited by the lifetime of the fluorescent probe.

Due to the complexity of Ca^{2+} homeostasis and signaling pathways, comprehensive analysis of toxicant-induced alterations to these mechanisms can be challenging. Many specific molecular targets (membrane receptors, channels, and second messengers) are needed for the propagation of Ca^{2+} oscillations or waves. Pharmacological probing of these targets allows the mechanistic dissection of individual cell-specific and toxicant-modulated pathways involved in Ca^{2+} signaling [4]. Evaluation of Ca^{2+} homeostasis in vitro can be performed with non-invasive imaging tools by use of a variety of strategies. Methodologies range from relatively simple steady state measurements of cytosolic and/or mitochondrial Ca^{2+} to more complex dynamic measurements of Ca^{2+} and Ca^{2+} signaling events induced by biological response modifiers that can be altered by toxicants. In the following section, the types of information that may be derived from different methods of analysis, including steady state, short-term kinetic (stimulated transient), and long-term kinetic measurements of Ca^{2+} homeostasis and signaling, are briefly discussed.

3. Model Cell Types and Neurotoxicants

Examples used to illustrate different methods of Ca^{2+} analysis are drawn from experiments with two main cell types. The first cell type selected is the astrocytoma cell line CCF-STTG1 established from a specimen of Grade IV astrocytoma, (ATCC, Manassas, VA), based on the ability of these cells to generate Ca^{2+} waves in response to stimulants such as fetal bovine serum (FBS) or adenosine 5'-triphosphate (ATP) and to exhibit differences in Ca^{2+} signaling when treated with different toxicants [5]. In addition, these cells do not exhibit connexin 43 and do not have gap junctions (unpublished observations). The second cell type is astrocytes in primary culture, which allow a degree of validation of results obtained from the astrocytoma cell line. In addition, we compared primary mouse astrocytes (wild type) and primary astrocyte cultures prepared from mice in which one copy of the neurofibromatosis type 1 gene product was ablated (*nf1*^{+/-}). Disruption of Ca^{2+} wave propagation has been reported in keratinocytes cultured from patients in which *nf1* is mutated, and is directly linked to the reduction of neurofibromin expression [36]. It is therefore of interest to examine the roles of neurofibromin in astrocyte Ca^{2+} signaling in a genetic model in which Ca^{2+} wave propagation may be disrupted.

Chemicals used as models for studying the different types of Ca^{2+} signaling described in this review included propofol (2,6-diisopropyl phenol; Disoprivan), valproic acid (VPA, 2-n-propylpentanoic acid), benzo-a-pyrene (BaP), benzo-e-pyrene (BeP), 5-methylchrysene (5-MeCr), lead and manganese. Propofol and VPA are two neuroactive drugs that have been investigated for cytotoxicity and biological responses in culture. They were selected as model compounds because they are neurotoxic to the developing nervous system in vivo. Propofol is a widely used intravenous general anesthetic that has also been used to provide long-term sedation for patients in intensive care units and is thought to have few side effects. In the central nervous system, propofol induces a dose-dependent suppression of awareness. Prolonged sedation with propofol may cause neurologic sequelae in children [39], [71], and [12] and short-term sedation may cause convulsions [24], [58] and [74]. The mechanisms of propofol action and potential toxicity have been studied in vitro; however, results have been conflicting (i.e.,

clinical levels may be without effect in some systems but not others, and different endpoints used among studies do not permit direct comparisons) [65].

VPA is an antiepileptic drug used in the US since 1978 [22]. Human brain concentrations of sodium valproate following 72 hours of therapy in nine neurosurgical patients were found to range from 6.8% to 27.9 % the blood concentration [73]. More recently, it has been used in the treatment of bipolar affective disorders [14] and migraine headaches [62]. Its clinical use is increasing, which increases the potential for associated toxicity and the need for further studies of its effects on Ca^{2+} homeostasis. Exposure to VPA at therapeutic doses during early pregnancy can cause neural tube defects in humans and in mice [49]. The mechanism of teratogenesis is unknown, though most toxicity is attributable to the parent compound, rather than a metabolite [48]. This factor renders the drug suitable for the proposed direct testing in vitro.

BeP, BaP and 5-MeC are polycyclic aromatic hydrocarbons (PAHs) that are persistent environmental pollutants. Human exposure to PAHs occurs primarily through the smoking of tobacco, inhalation of polluted air, and ingestion of food and water contaminated by combustion effluents. The effects of diol epoxide metabolites of PAHs on $[\text{Ca}^{2+}]_i$ may also play a role in tumorigenesis [32]. Numerous epidemiologic studies have shown a clear association between exposure to various mixtures of PAHs containing BaP and increased risk of cancer [68]. BeP is structurally very similar to BaP, but unlike BaP it is a weak aryl hydrocarbon receptor ligand and has a weak or no carcinogenic activity [15] and [9]. This makes BeP an ideal negative control for use in addition to regular vehicle controls in experiments. Recent evidence suggests that disruption of cellular signaling pathways and cellular homeostasis can contribute significantly to the toxicity of BaP [4]. BaP also induces, through cytochrome P450-dependent metabolism, a dose-dependent increase in intracellular Ca^{2+} in the human mammary epithelial cell line MCF-10A [66], and apoptosis in B cells via Ca^{2+} -dependent mechanisms [56]. In general, a strong association exists between PAHs and changes in Ca^{2+} homeostasis [37]

Lead is an environmental neurotoxicant that has been well studied in vitro. The blood and brain level of lead can be higher than 10 $\mu\text{g}/\text{ml}$ and 3 $\mu\text{g}/\text{ml}$ respectively in some cases [18] and long term exposure has been suggested as a risk factor in the development of Parkinson's disease [17]. Many effects of lead on neuronal and glial cultured cells have been reported such as altered glutamate metabolism [59], altered calcium homeostasis [57], oxidative or mitochondrial stress and reduced basal respiratory rate [30] and [40].

Manganese is also an environmental neurotoxicant. Low levels of manganese are present in water and food, and occupational exposures can occur with inhalation of manganese particulates from welding [33]. Manganese has been shown to inhibit Na-dependent Ca^{2+} efflux [26] and respiration in brain mitochondria [76] both of which are necessary to maintain ATP as well as Ca^{2+} levels.

4. Methods for Measurements of Intracellular Ca^{2+}

4.1. Steady State Measurements

4.1.1 Cytosolic and mitochondrial Ca^{2+} concentrations—A simple measurement of cellular health is the steady state ratio of cytosolic to mitochondrial $[\text{Ca}^{2+}]$. Steady state measurements of cytosolic and mitochondrial Ca^{2+} concentrations are straight forward and can be useful to evaluate perturbations of Ca^{2+} homeostasis that result when the ON and OFF mechanisms (Figure 1) are compromised. $[\text{Ca}^{2+}]_i$ regulation is compromised if the OFF mechanisms cannot keep pace with Ca^{2+} influx in a toxicant-challenged cell, i.e., when the capacity to transfer cytosolic Ca^{2+} to the endoplasmic reticulum, mitochondria and/or the

extracellular space is exceeded. When cytosolic Ca^{2+} levels remain elevated for an extended period of time, mitochondrial Ca^{2+} levels increase to pathological levels. This increase can lead to depolarization of mitochondria and cell death.

Probes for monitoring cytosolic Ca^{2+} include fura-2, indo-1, fluo-4, and others. In addition, fluo-5F, fluo-4FF, fluo-5N and mag-fluo-4 can be used for measuring Ca^{2+} levels in endoplasmic reticulum (ER) and rhod-2 can be used for mitochondrial Ca^{2+} levels. Fura-2 is a ratiometric probe with dual excitation wavelengths of 340 nm (Ca^{2+} -bound) and 380 nm (Ca^{2+} -free) and an emission wavelength of 510 nm. The shift in wavelength upon binding of Ca^{2+} by the dye is independent of Ca^{2+} concentrations within physiological limits, and thus fura-2 allows accurate measurements of Ca^{2+} concentrations. Indo-1 is also a ratiometric probe that allows sensitive quantification of Ca^{2+} concentrations. When indo-1 is excited at 350 nm, its emission wavelength shifts from 475 nm to 400 nm upon binding to Ca^{2+} . In contrast to fura-2 and indo-1, fluo-4 is excited by visible light (close to 488 nm), is nonfluorescent, and becomes fluorescent upon binding to Ca^{2+} at one emission wavelength (close to 510 nm). Fluo-4 provides higher signal levels than fura-2 or indo-1 for confocal microscopy and high-throughput screening, such as microplate assays, because it exhibits a large fluorescence intensity increase upon binding Ca^{2+} . However, because it is a nonratiometric dye that does not exhibit a spectral shift upon binding to Ca^{2+} , fluo-4 is less useful than the other dyes for quantitative Ca^{2+} measurements but more useful for measuring relative changes in dynamic Ca^{2+} measurements. Its analogs fluo-5F, fluo-4FF, and fluo-5N have lower Ca^{2+} -binding affinities than fluo-4, and are thus useful for detecting Ca^{2+} in environments with high Ca^{2+} levels that would saturate fluo-4, such as the ER. Rhod-2 is a long wavelength Ca^{2+} fluorophore with excitation and emission maxima at 552 nm and 581 nm, respectively. It is a cationic dye that is taken up by mitochondria. Cytosolic and mitochondrial Ca^{2+} concentrations can be measured simultaneously in cells loaded with fluo-4 and rhod-2, as both are excited by visible light and their emission maxima are sufficiently distinct to allow separate collection of their signals.

Simultaneous evaluation of cytosolic and mitochondrial Ca^{2+} levels (Figure 2) is a particularly useful combination for steady state measurements. The choice of fluorescent probes depends on the type of information desired (quantitative or qualitative data) and must be matched with a suitable combination of filter sets used on a particular instrument for measuring excitation and emission spectra of these probes. In addition, the probe choice should be tested with the toxicant or treatment under investigation to avoid any possible interactions between the two [67]. For example, interactions have been seen between Ca^{2+} probes and metals such as Pb^{2+} or Mg^{2+} [41] and [44]. Most of the examples presented in this report were performed with either fluo-4 for measuring cytosolic Ca^{2+} or a combination of fluo-4 and rhod-2 for measuring cytosolic Ca^{2+} and mitochondrial Ca^{2+} concentrations, as well as the ratio of mitochondrial to cytosolic [Ca^{2+}].

Steady state cytosolic and mitochondrial Ca^{2+} measurements in cultured cells exposed for some interval to a specific treatment can be evaluated by a simple calculation of mean fluorescence intensity of the Ca^{2+} -sensitive probe. The ratio (R) of mitochondrial to cytosolic [Ca^{2+}] can be a more sensitive parameter for quantification of Ca^{2+} variations in cells than either value alone [26], [4] and [42]. Examples of this type of measurement are shown in Figure 3. In these examples, propofol and VPA were selected as models for study because their neurotoxic mechanisms may involve altered Ca^{2+} homeostasis [34], [25], [75] and [43]. The two drugs were initially screened for cytotoxicity following 24 or 72 hrs exposure to a range of concentrations that included therapeutic levels. Concentrations of propofol were tested that are close to 20 μM , the steady state blood concentration of propofol in children treated with this anesthetic is [45]. Therapeutic concentrations of propofol in human brain have not been reported. The data revealed that propofol causes a concentration-dependent decrease in cell

viability: the concentrations that inhibit cell viability by 50% (IC₅₀) relative to controls are $14 \pm 0.5 \mu\text{M}$ at 24 h and $27 \pm 3.0 \mu\text{M}$ at 72 h [5]. The higher IC₅₀ after exposure for 72 h may have resulted from detachment of non-viable cells, which were lost from the cultures when they were rinsed, and an adaptive response to propofol. In contrast, VPA was non-cytotoxic at 1-4 mM (data not shown), where 1mM is close to therapeutic levels [20]. In the example shown in Figure 3, mitochondrial Ca²⁺ levels significantly increased while cytoplasmic Ca²⁺ levels decreased at a propofol concentration (1 μM for 72 h) which is much lower than the IC₅₀ (27 μM). The ratio of mitochondrial to cytosolic [Ca²⁺] exhibited a significant increase in propofol-treated cells. In contrast, VPA treatment had no effect, supporting its lack of cytotoxicity in this experimental paradigm. This simple analysis of mitochondrial to cytosolic [Ca²⁺] demonstrates that propofol and VPA have distinct effects on Ca²⁺ homeostasis in CCF-STTG1 cells, but offers no detailed information on the mechanisms of action of either drug.

A better understanding of the mechanism of the propofol effect on steady state [Ca²⁺]_i in CCF-STTG1 cells can be achieved with specific pharmacologic agents. In the example shown in Figure 2C, diazoxide, a mitochondrial ATP-dependent K⁺ channel activator was used to probe involvement of these channels in CCF-STTG1 cells. We found that in cells exposed for 72 h to 20 μM propofol, treatment with 10 μM diazoxide for 1 h prior to imaging reverses the increase in the ratio of mitochondrial to cytosolic [Ca²⁺]. This finding indicates the activation of mitochondrial ATP-dependent K⁺ channels by propofol treatment (Figure 2C).

4.1.2 Strengths and limitations of steady state measurements—Steady state measurements of global cytosolic and mitochondrial Ca²⁺ levels are easy to perform and interpret. They are carried out at a single time point and are amenable for use in single whole cells, as well as groups of cells. Steady state measurements are therefore useful for obtaining data from a population of cells. Although static Ca²⁺ levels are the easiest parameter to measure as an indicator of Ca²⁺ homeostasis, and the most amenable to high throughput screening assays, the information they provide is limited. Static measurements do not provide detailed information on mechanisms of toxic action. Though they detect positives readily, they may produce false negatives by missing more subtle positives. Thus, cells may be damaged and their Ca²⁺ regulatory mechanisms impaired without detectable effects on steady state cytosolic and mitochondrial Ca²⁺ measurements. Therefore, even in the face of potentially correct negatives, it is reasonable to follow up static measurements with dynamic measurements of Ca²⁺ homeostasis.

In addition to the advantages and drawbacks of steady state measurements as discussed, the choice of fluorophores contributes its own set of strengths and limitations. Nonratiometric Ca²⁺-sensitive fluorophores such as fluo-4 and rhod-2 are convenient to use because they can be loaded easily into cells in the acetoxymethyl form and their excitation and emission maxima are in the visible range. Both of these dyes are bright and are accurate for recording relative changes in intensity compared to the basal level. However, quantification of specific intracellular Ca²⁺ levels is less precise with nonratiometric probes than with ratiometric probes. Another drawback of nonratiometric Ca²⁺ probes is that they are more sensitive to cell variabilities in the extent of dye loading and photobleaching. However, the expression of cytosolic and mitochondrial Ca²⁺ data obtained with fluo-4 and rhod-2 as a ratio eliminates variables that might arise from cytosolic fluorophore concentration, cell size, cell shape, and cell number [52]. In this manner, fluo-4 and rhod-2 can be used as ratiometric dyes.

4.2. Short-term kinetic measurements of stimulated Ca²⁺ transients

4.2.1 Stimulated Ca²⁺ transients—A more sophisticated approach to analyzing the mechanistic effects of a toxicant on Ca²⁺ homeostasis is to probe the effects of the toxicant on the Ca²⁺ transient. Several types of stimulants can be used to induce a transient increase in

$[Ca^{2+}]_i$ that can be monitored for up to five minutes, such as hormones, ATP, and mechanical stimulation. This type of short term kinetic analysis allows a more detailed probing of the individual contributions of membrane ion channels on the ER and plasma membrane to a toxic response. As an example, further analysis of $[Ca^{2+}]_i$ was carried out in propofol-treated CCF-STTG1 cells stimulated with fetal bovine serum (FBS). In control cells, FBS stimulates a rapid increase in cytosolic $[Ca^{2+}]_i$ that returns to baseline within several minutes. Propofol significantly decreases the amplitude of this Ca^{2+} transient. Use of several pharmacological agents to try to reverse or block the propofol effect on this Ca^{2+} transient helped identify a VOC channel opener (Bay-K 8644) that can reverse this effect. This result, together with the previously mentioned reversal by diazoxide of the propofol effect on the ratio of mitochondrial to cytosolic and $[Ca^{2+}]_i$, identified two specific molecular effects of propofol: the deactivation of L-type VOC channels and the activation of mitochondrial K^+ -ATP channels [5].

Returning to the possibility that steady state measurements may produce false negatives, we conducted short-term kinetic measurements of stimulated Ca^{2+} transients in CCF-STTG1 cells treated with VPA. VPA had no effect on FBS-induced transient Ca^{2+} response (data not shown). This result, like the steady state measurements previously described, supports the conclusion that propofol and VPA have different mechanisms of toxicity but does not yet rule out possible effects of VPA on Ca^{2+} signaling.

4.2.2 Strengths and limitations of short-term kinetic measurements of stimulated Ca^{2+} transients—Short-term global kinetic measurements may provide additional information to supplement steady state $[Ca^{2+}]_i$ measurements. Data are acquired by measuring cytosolic $[Ca^{2+}]_i$ in a whole cell or group of cells at multiple time points for several minutes after stimulating a global Ca^{2+} transient. The effect of a toxicant on the amplitude of the transient can be observed, and pharmacological agents that affect specific ON or OFF switches can be tested in order to identify mechanisms affected by the toxicant. Short term kinetic measurements of stimulated $[Ca^{2+}]_i$ transients are useful for obtaining population data. Similar to the ratio (R) of mitochondrial to cytosolic $[Ca^{2+}]_i$, the short time transient response may detect mechanistic differences between the actions of two toxicants on a cell but may also produce false negatives. Because of this limitation, stimulation of complex intracellular Ca^{2+} responses involving multiple signaling pathways would be a motif for applying more powerful, dynamic measurements of Ca^{2+} signaling and homeostasis to further investigate chemical or toxicant effects. The ultimate goal of dynamic measurements, which will be discussed in the next section, is to develop a model that includes all targets affected by toxicant and identify them with help of specific inhibitors and activators.

4.3. Dynamic Measurements of Cellular Ca^{2+}

4.3.1 Ca^{2+} Waves and Oscillations—Dynamic Ca^{2+} measurements can be monitored in cells exposed to toxicant treatments for a fixed interval followed by stimulation of cells with a hormone, neurotransmitter, mechanical stimulus or other biological response modifier to initiate, intracellular Ca^{2+} waves or oscillations and intercellular Ca^{2+} waves. Analysis of intercellular Ca^{2+} waves usually involves the measurement of the average wave velocity, amplitude and width [38] and [69]. Wave velocities vary from 0.1-1 $\mu\text{m}/\text{sec}$ (slow) to 10-50 $\mu\text{m}/\text{sec}$ (fast) [31]. Another useful method to analyze waves is to dissect the stimulant-induced global Ca^{2+} response into 3 separate parameters (Figure 4):

- a. Half-life is the term used to describe half of the duration of any given wave. This parameter indirectly gives the length of time a wave will last before it disappears.
- b. Rate of the wave describes the speed by which the Ca^{2+} signal propagates within and/or between cells.

- c. Span of the wave identifies differences between the starting and ending amplitude of a wave.

The decay in fluorescence intensity is due to the disappearance of the wave and not photobleaching, as acquisition parameters were adjusted to minimize photobleaching to less than 5% of the total signal.

Data in Figures 5 illustrate specific effects of several chemical treatments on the parameters of the Ca^{2+} wave. Figure 5A illustrates the changes in half-life, rate, of the Ca^{2+} wave in CCF-STTG1 cells treated with propofol (0, 20 μM) for 72 hrs. In this case, propofol reduced the half-life of the wave, increased the rate of wave propagation and had no effect on the wave span (data not shown). Another example of wave analysis is shown in Figure 4B where CCF-STTG1 cells were treated with different concentrations of valproic acid (0, 1, 2, 4 mM) for 72 hrs. Significant changes in wave propagation were also observed with VPA treated cells only at high concentration (4 mM). The reduced half-life and increased rate of the wave may be linked to ATP production necessary for wave propagation. A decrease in half-life and increase in rate were observed in the same cell type exposed to Pb and Mn (Figure 5C and 5D). Another example (Figure 6) shows the wave analysis applied to primary astrocytes from wild type and *nfl* mutant mice. This example shows that neurofibromin has a significant effect only on the rate of the wave. Because neurofibromin increases ATP production [51] and [70] and propofol, valproic acid, and manganese decrease ATP production [5], [42] and [13], the above examples correlate well with this data demonstrating that the wave analysis may be directly linked to ATP production and can be used as an indicator for analysis of significant alteration in ATP production. In summary, the wave analysis method indicates that reproducible measurements of chemically-induced changes in Ca^{2+} waves can be made in cultured cells and that individual toxicants can give rise to a signature pattern of altered Ca^{2+} responses.

While the analysis of Ca^{2+} waves is performed by evaluating the parameters listed above, analysis of Ca^{2+} oscillations can be enhanced by incorporating additional steps that include transformation of the signal from the time domain to the frequency domain. When the Ca^{2+} oscillations are uniform or stationary (Figure 7), the analysis can be accomplished by Fast Fourier Transform (FFT) that will identify the frequency as well as the amplitude of these oscillations [[72]. Figure 7A shows an example of oscillations induced by 20 nM oxytocin in a uterine smooth muscle (myometrial) cell type. These oscillations, which were monitored for approximately 2 hrs [4], exhibit a uniform frequency observed between 40 and 80 min following treatment with oxytocin. FFT was applied to this oscillatory signal to determine the frequency and amplitude (Figure 7B). When the Ca^{2+} oscillations are not stationary, FFT may be used to identify the frequencies present in a Ca^{2+} signal. However, Wavelet Transform would be the method of choice to identify the time at which these frequencies occurred [29]. We first developed the FFT technique to analyze oxytocin-induced oscillatory Ca^{2+} signals in liver and myometrial cell types in order to identify mechanisms of toxicity of BaP [6] and [4]. In the myometrial cell line, BaP was found to alter oxytocin-induced Ca^{2+} oscillations by altering the receptor tyrosine kinase pathway, membrane channels, and PKC activity. Use of receptor tyrosine kinase activators such as serum or EGF primarily restore the function of the tyrosine kinase pathway and secondarily restore membrane channels and PKC activity, thereby reversing the effects of BaP on the frequency of oxytocin-induced Ca^{2+} oscillations.

FFT is particularly valuable when multiple treatment effects must be assessed. For example, a similar FFT analysis in CCF-STTG1 cells treated with BaP, 5-MeCr, and a binary mixture of BaP and 5-MeCr for 24 hrs, revealed that BaP and 5-MeCr alone or in a binary mixture induced a significant decrease in the frequency of Ca^{2+} oscillations (Figure 8), as well as a significant decrease in the number of cells exhibiting Ca^{2+} oscillations (data not shown). In addition, full restoration of Ca^{2+} oscillations in CCF-STTG1 cells was achieved (Figure 8, bottom panel) with the same chemical interventions applied to BaP-treated myometrial cells,

i.e., the use of EGF and barium acetate or tetraethylammonium to restore receptor tyrosine kinase activity and K^+ channel function. These results indicate that BaP and 5-MeC exert their effects through the same mechanisms in myometrial cells and CCF-STTG1 cells. It is important to note that BeP had no effect on the frequency of Ca^{2+} oscillations (data not shown).

For both types of dynamic measurements (Ca^{2+} waves or oscillations), a mathematical model comprised of equations representing the different ON and OFF pathways (including receptor activation, signaling steps, and feed-back loops involved in regulating Ca^{2+} levels within different intracellular compartments) may be developed and used to identify the contribution of each parameter in the complex Ca^{2+} signal generated by neurotransmitter or hormone stimulation. Such models [10], [19], [21], [23] and [63], once established for each cell type, may be used to determine the source of altered Ca^{2+} signal induced by toxicant treatment.

4.3.2. Strengths and limitations of dynamic measurements—As mentioned earlier, global Ca^{2+} transients can propagate through the cell as waves, adding a spatial dimension to analysis of Ca^{2+} homeostasis. Ca^{2+} waves may also be propagated repetitively as $[Ca^{2+}]_i$ oscillations of uniform frequency. Dynamic measurements of Ca^{2+} waves and oscillations can be made in time and space. Dynamic measurements involving Ca^{2+} oscillations or waves require extended periods of data collection (minutes to hours) and the use of inhibitors and activators of specific ON and OFF pathways in order to construct a model for a specific cell type. Dynamic measurements of waves involve more extensive mathematical analysis than steady state and short term kinetic analyses. They are necessary for the analysis of oscillations and they require complex mathematical modeling with non-linear differential equations. However, once the model for a given cell and toxicant is built, the benefits will be enormous as one can dissect the specific effects of a biological response modifier on cellular Ca^{2+} homeostasis and signaling machinery. It then becomes possible to more rapidly screen and compare the action of a variety of toxicants and biological response modifiers to the unexposed control sample. Image analysis of Ca^{2+} signaling in multiple samples and mathematical modeling of normal Ca^{2+} responses are amenable to automation and could be extended to high throughput analysis of potential neurotoxicants.

5. Conclusions

Abnormal spatial and temporal alterations in Ca^{2+} signaling occur in cells exposed to toxicants, as well as in cells in numerous disease states. Methodologies for detecting and analyzing subtle alterations in real time with non-invasive imaging tools are becoming increasingly refined. These methods include comprehensive analyses of both steady state and dynamic Ca^{2+} levels, partitioning of Ca^{2+} between the cytosol and mitochondria, and assessment of the functional status of specific molecular components that maintain basal ($[Ca^{2+}]_i$) or that take part in the propagation of Ca^{2+} oscillations or waves.

There is no single bioassay or risk assessment strategy that can be used for toxicity assessment of toxicants. In our hands, non-invasive imaging tools in conjunction with fluorescent biomarkers and biosensors of cellular function have proven useful for investigating mechanisms of toxicant action in culture systems. It has also been possible to identify specific cellular targets of injury and restore the function of these targets in cultured cells. However, it is important that mechanistic data derived from cultured cells be useful for translation to the context of the biological complexity of tissue and organ histoarchitecture (multiple cell types receiving complex signals in a three dimensional matrix) and numerous other confounding factors such as genetic susceptibility, nutrition/health of the exposed individual, and the duration and timing of exposure, to name a few. An understanding of individual Ca^{2+} signaling pathways that are targeted by specific toxicants provides a better screening for more complex mechanistic analysis of cellular injury. The tools and approaches described in this perspective

paper produce reliable measurements that can be applied to high throughput organ- and tissue-level assessment of cellular responses caused by toxicants.

Acknowledgments

Calcium imaging performed in the College of Veterinary Medicine & Biomedical Sciences Image Analysis Laboratory, was supported by NIH-NCRR (1 S10 RR22532-01), and NIH-NIEHS grants P30-ES09106, P42-ES04917 and T32 ES07273. Propofol and VPA research was also supported by a Colgate-Palmolive grant for Alternative Research.

References

- [1]. Abdullaev IF, Bisaillon JM, Potier M, Gonzalez JC, Motiani RK, Trebak M. Stim1 and Orai1 mediate CRAC currents and store-operated calcium entry important for endothelial cell proliferation. *Circ Res* 2008;103:1289–99. [PubMed: 18845811]
- [2]. Albrecht J, Matyja E. Glutamate: a potential mediator of inorganic mercury neurotoxicity. *Metab Brain Dis* 1996;11:175–84. [PubMed: 8776719]
- [3]. Atchison WD, Hare MF. Mechanisms of methylmercury-induced neurotoxicity. *Faseb J* 1994;8:622–9. [PubMed: 7516300]
- [4]. Barhoumi R, Awooda I, Mouneimne Y, Safe S, Burghardt RC. Effects of benzo-a-pyrene on oxytocin-induced Ca²⁺ oscillations in myometrial cells. *Toxicol Lett* 2006;165:133–41. [PubMed: 16567066]
- [5]. Barhoumi R, Burghardt RC, Qian Y, Tiffany-Castiglioni E. Effects of propofol on intracellular Ca²⁺ + homeostasis in human astrocytoma cells. *Brain Res* 2007;1145:11–8. [PubMed: 17328872]
- [6]. Barhoumi R, Faske J, Liu X, Tjalkens RB. Manganese potentiates lipopolysaccharide-induced expression of NOS2 in C6 glioma cells through mitochondrial-dependent activation of nuclear factor kappaB. *Brain Res Mol Brain Res* 2004;122:167–79. [PubMed: 15010209]
- [7]. Barhoumi R, Mouneimne Y, Awooda I, Safe SH, Donnelly KC, Burghardt RC. Characterization of calcium oscillations in normal and benzo[a]pyrene-treated clone 9 cells. *Toxicol Sci* 2002;68:444–50. [PubMed: 12151640]
- [8]. Berridge MJ, Bootman MD, Roderick HL. Calcium signalling: dynamics, homeostasis and remodelling. *Nat Rev Mol Cell Biol* 2003;4:517–29. [PubMed: 12838335]
- [9]. Bigelow SW, Nebert DW. The Ah regulatory gene product. Survey of nineteen polycyclic aromatic compounds' and fifteen benzo[a]pyrene metabolites' capacity to bind to the cytosolic receptor. *Toxicol Lett* 1982;10:109–18. [PubMed: 7080063]
- [10]. Boitier E, Rea R, Duchen MR. Mitochondria exert a negative feedback on the propagation of intracellular Ca²⁺ waves in rat cortical astrocytes. *J Cell Biol* 1999;145:795–808. [PubMed: 10330407]
- [11]. Bootman MD, Collins TJ, Peppiatt CM, Prothero LS, MacKenzie L, De Smet P, Travers M, Tovey SC, Seo JT, Berridge MJ. Calcium signalling--an overview. *Semin Cell Dev Biol* 2001;12:3–10. others. [PubMed: 11162741]
- [12]. Bray RJ. Propofol infusion for ICU sedation in children. *Anaesthesia* 2002;57:521. [PubMed: 12004826]
- [13]. Brouillet EP, Shinobu L, McGarvey U, Hochberg F, Beal MF. Manganese injection into the rat striatum produces excitotoxic lesions by impairing energy metabolism. *Exp Neurol* 1993;120:89–94. [PubMed: 8477830]
- [14]. Calabrese JR, Delucchi GA. Spectrum of efficacy of valproate in 55 patients with rapid-cycling bipolar disorder. *Am J Psychiatry* 1990;147:431–4. [PubMed: 2107762]
- [15]. Carlson EA, Li Y, Zelikoff JT. Benzo[a]pyrene-induced immunotoxicity in Japanese medaka (*Oryzias latipes*): relationship between lymphoid CYP1A activity and humoral immune suppression. *Toxicol Appl Pharmacol* 2004;201:40–52. [PubMed: 15519607]
- [16]. Casares FM, Mantione K. Pesticides may be altering constitutive nitric oxide release, thereby compromising health. *Med Sci Monit* 2006;12:RA235–40. [PubMed: 17006416]

- [17]. Coon S, Stark A, Peterson E, Gloi A, Kortsha G, Pounds J, Chettle D, Gorell J. Whole-body lifetime occupational lead exposure and risk of Parkinson's disease. *Environ Health Perspect* 2006;114:1872–6. [PubMed: 17185278]
- [18]. Cremin JD Jr, Smith DR. In vitro vs in vivo Pb effects on brain protein kinase C activity. *Environ Res* 2002;90:191–9. [PubMed: 12477464]
- [19]. Cuthbertson KS, Chay TR. Modelling receptor-controlled intracellular calcium oscillators. *Cell Calcium* 1991;12:97–109. [PubMed: 1647879]
- [20]. Cuturic M, Abramson RK. Acute hyperammonemic coma with chronic valproic acid therapy. *Ann Pharmacother* 2005;39:2119–23. [PubMed: 16288075]
- [21]. Dupont G, Goldbeter A. One-pool model for Ca²⁺ oscillations involving Ca²⁺ and inositol 1,4,5-trisphosphate as co-agonists for Ca²⁺ release. *Cell Calcium* 1993;14:311–22. [PubMed: 8370067]
- [22]. Eadie MJ, Hooper WD, Dickinson RG. Valproate-associated hepatotoxicity and its biochemical mechanisms. *Med Toxicol Adverse Drug Exp* 1988;3:85–106. [PubMed: 3131628]
- [23]. Falcke M, Or-Guil M, Bar M. Dispersion gap and localized spiral waves in a model for intracellular Ca²⁺ dynamics 2000. *Phys Rev Lett* 2000;84:4753–6. [PubMed: 10990788]
- [24]. Finley GA, MacManus B, Sampson SE, Fernandez CV, Retallick R. Delayed seizures following sedation with propofol. *Can J Anaesth* 1993;40:863–5. [PubMed: 8403180]
- [25]. Garib V, Lang K, Niggemann B, Zanker KS, Brandt L, Dittmar T. Propofol-induced calcium signalling and actin reorganization within breast carcinoma cells. *Eur J Anaesthesiol* 2005;22:609–15. [PubMed: 16119598]
- [26]. Gavin CE, Gunter KK, Gunter TE. Manganese and calcium efflux kinetics in brain mitochondria. Relevance to manganese toxicity. *Biochem J* 1990;266:329–34. [PubMed: 2317189]
- [27]. Gu X, Spitzer NC. Distinct aspects of neuronal differentiation encoded by frequency of spontaneous Ca²⁺ transients. *Nature* 1995;375:784–7. [PubMed: 7596410]
- [28]. Hajnoczky G, Robb-Gaspers LD, Seitz MB, Thomas AP. Decoding of cytosolic calcium oscillations in the mitochondria. *Cell* 1995;82:415–24. [PubMed: 7634331]
- [29]. Hasty J, Collins JJ, Wiesenfeld K, Grigg P. Wavelets of excitability in sensory neurons. *J Neurophysiol* 2001;86:2097–101. [PubMed: 11600664]
- [30]. Holtzman D, Olson JE, DeVries C, Bensch K. Lead toxicity in primary cultured cerebral astrocytes and cerebellar granular neurons. *Toxicol Appl Pharmacol* 1987;89:211–25. [PubMed: 3603558]
- [31]. Jaffe LF, Creton R. On the conservation of calcium wave speeds. *Cell Calcium* 1998;24:1–8. [PubMed: 9793683]
- [32]. Jyonouchi H, Sun S, Porter VA, Cornfield DN. Polycyclic aromatic hydrocarbon diol epoxides increase cytosolic Ca(2+) of airway epithelial cells. *Am J Respir Cell Mol Biol* 2001;25:78–83. [PubMed: 11472978]
- [33]. Keen CL, Ensunsa JL, Clegg MS. Manganese metabolism in animals and humans including the toxicity of manganese. *Met Ions Biol Syst* 2000;37:89–121. [PubMed: 10693132]
- [34]. Kim HS, Chang WC, Hwang KC, Choi IG, Park WK. Effect of propofol on calcium homeostasis in hypoxia-reoxygenated neonatal rat cardiomyocytes. *Eur J Pharmacol*. 2008
- [35]. Kolar SS, Barhoumi R, Lupton JR, Chapkin RS. Docosahexaenoic acid and butyrate synergistically induce colonocyte apoptosis by enhancing mitochondrial Ca²⁺ accumulation. *Cancer Res* 2007;67:5561–8. [PubMed: 17545640]
- [36]. Korkiamaki T, Yla-Outinen H, Koivunen J, Karvonen SL, Peltonen J. Altered calcium-mediated cell signaling in keratinocytes cultured from patients with neurofibromatosis type 1. *Am J Pathol* 2002;160:1981–90. [PubMed: 12057903]
- [37]. Krieger JA, Davila DR, Lytton J, Born JL, Burchiel SW. Inhibition of sarcoplasmic/endoplasmic reticulum calcium ATPases (SERCA) by polycyclic aromatic hydrocarbons in HPB-ALL human T cells and other tissues. *Toxicol Appl Pharmacol* 1995;133:102–8. [PubMed: 7597699]
- [38]. Kupferman R, Mitra PP, Hohenberg PC, Wang SS. Analytical calculation of intracellular calcium wave characteristics. *Biophys J* 1997;72:2430–44. [PubMed: 9168020]
- [39]. Lanigan C, Sury M, Bingham R, Howard R, Mackersie A. Neurological sequelae in children after prolonged propofol infusion. *Anaesthesia* 1992;47:810–1. [PubMed: 1415983]

- [40]. Legare ME, Barhoumi R, Burghardt RC, Tiffany-Castiglioni E. Low-level lead exposure in cultured astroglia: identification of cellular targets with vital fluorescent probes. *Neurotoxicology* 1993;14:267–72. [PubMed: 8247400]
- [41]. Legare ME, Barhoumi R, Hebert E, Bratton GR, Burghardt RC, Tiffany-Castiglioni E. Analysis of Pb²⁺ entry into cultured astroglia. *Toxicol Sci* 1998;46:90–100. [PubMed: 9928672]
- [42]. Luis PB, Ruiten JP, Aires CC, Soveral G, de Almeida IT, Duran M, Wanders RJ, Silva MF. Valproic acid metabolites inhibit dihydrolipoyl dehydrogenase activity leading to impaired 2-oxoglutarate-driven oxidative phosphorylation. *Biochim Biophys Acta* 2007;1767:1126–33. [PubMed: 17706936]
- [43]. Manning TJ Jr. Sontheimer H. Spontaneous intracellular calcium oscillations in cortical astrocytes from a patient with intractable childhood epilepsy (Rasmussen's encephalitis). *Glia* 1997;21:332–7. [PubMed: 9383042]
- [44]. Marchi B, Burlando B, Panfoli I, Viarengo A. Interference of heavy metal cations with fluorescent Ca²⁺ probes does not affect Ca²⁺ measurements in living cells. *Cell Calcium* 2000;28:225–31. [PubMed: 11032778]
- [45]. McFarlan CS, Anderson BJ, Short TG. The use of propofol infusions in paediatric anaesthesia: a practical guide. *Paediatr Anaesth* 1999;9:209–16. [PubMed: 10320599]
- [46]. Monga M, Ku CY, Dodge K, Sanborn BM. Oxytocin-stimulated responses in a pregnant human immortalized myometrial cell line. *Biol Reprod* 1996;55:427–32. [PubMed: 8828850]
- [47]. Morken TS, Sonnewald U, Aschner M, Syversen T. Effects of methylmercury on primary brain cells in mono- and co-culture. *Toxicol Sci* 2005;87:169–75. [PubMed: 15958655]
- [48]. Nau H. Species differences in pharmacokinetics and drug teratogenesis. *Environ Health Perspect* 1986;70:113–29. [PubMed: 3104022]
- [49]. Nau H, Hauck RS, Ehlers K. Valproic acid-induced neural tube defects in mouse and human: aspects of chirality, alternative drug development, pharmacokinetics and possible mechanisms. *Pharmacol Toxicol* 1991;69:310–21. [PubMed: 1803343]
- [50]. Niggli E, Shirokova N. A guide to sparkology: the taxonomy of elementary cellular Ca²⁺ signaling events. *Cell Calcium* 2007;42:379–87. [PubMed: 17428535]
- [51]. Papa S. The NDUFS4 nuclear gene of complex I of mitochondria and the cAMP cascade. *Biochim Biophys Acta* 2002;1555:147–53. [PubMed: 12206907]
- [52]. Qian Y, Venkatraj J, Barhoumi R, Pal R, Datta A, Wild JR, Tiffany-Castiglioni E. Comparative non-cholinergic neurotoxic effects of paraoxon and diisopropyl fluorophosphate (DFP) on human neuroblastoma and astrocytoma cell lines. *Toxicol Appl Pharmacol* 2007;219:162–71. [PubMed: 17223147]
- [53]. Raheja G, Gill KD. Calcium homeostasis and dichlorvos induced neurotoxicity in rat brain. *Mol Cell Biochem* 2002;232:13–8. [PubMed: 12030370]
- [54]. Reither G, Schaefer M, Lipp P. PKC α : a versatile key for decoding the cellular calcium toolkit. *J Cell Biol* 2006;174:521–33. [PubMed: 16893971]
- [55]. Rose HJ, Dargan S, Shuai J, Parker I. 'Trigger' events precede calcium puffs in *Xenopus* oocytes. *Biophys J* 2006;91:4024–32. [PubMed: 16980363]
- [56]. Salas VM, Burchiel SW. Apoptosis in Daudi human B cells in response to benzo[a]pyrene and benzo[a]pyrene-7,8-dihydrodiol. *Toxicol Appl Pharmacol* 1998;151:367–76. [PubMed: 9707513]
- [57]. Sandhir R, Gill KD. Alterations in calcium homeostasis on lead exposure in rat synaptosomes. *Mol Cell Biochem* 1994;131:25–33. [PubMed: 8047062]
- [58]. Shah, PSSV. Propofol for procedural sedation/analgesia in neonates (Protocol). 2008 Edition. John Wiley & Sons, Ltd.; Jul 16. 2008
- [59]. Sierra EM, Tiffany-Castiglioni E. Reduction of glutamine synthetase activity in astroglia exposed in culture to low levels of inorganic lead. *Toxicology* 1991;65:295–304. [PubMed: 1671539]
- [60]. Skupin A, Kettenmann H, Winkler U, Wartenberg M, Sauer H, Tovey SC, Taylor CW, Falcke M. How does intracellular Ca²⁺ oscillate: by chance or by the clock? *Biophys J* 2008;94:2404–11. [PubMed: 18065468]
- [61]. Slegers H, Joniau M. Lipopolysaccharide-enhanced expression of interleukin-6 in dibutyryl cyclic AMP-differentiated rat C6 glioma. *J Neurochem* 1996;66:466–73. [PubMed: 8592115]

- [62]. Sneyd J, Charles AC, Sanderson MJ. A model for the propagation of intercellular calcium waves. *Am J Physiol* 1994;266:C293–302. [PubMed: 8304425]
- [63]. Sneyd J, Keizer J, Sanderson MJ. Mechanisms of calcium oscillations and waves: a quantitative analysis. *FASEB J* 1995;9:1463–72. [PubMed: 7589988]
- [64]. Spahr-Schopfer I, Vutskits L, Toni N, Buchs PA, Parisi L, Muller D. Differential neurotoxic effects of propofol on dissociated cortical cells and organotypic hippocampal cultures. *Anesthesiology* 2000;92:1408–17. [PubMed: 10781288]
- [65]. Tannheimer SL, Lauer FT, Lane J, Burchiel SW. Factors influencing elevation of intracellular Ca²⁺ in the MCF-10A human mammary epithelial cell line by carcinogenic polycyclic aromatic hydrocarbons. *Mol Carcinog* 1999;25:48–54. [PubMed: 10331744]
- [66]. Tepikin, A. Calcium signalling : a practical approach. Editoin Edition. Oxford University Press; Oxford ; New York: 2001.
- [67]. Thyssen J, Althoff J, Kimmerle G, Mohr U. Inhalation studies with benzo[a]pyrene in Syrian golden hamsters. *J Natl Cancer Inst* 1981;66:575–7. [PubMed: 6937711]
- [68]. Tjalkens RB, Zoran MJ, Mohl B, Barhoumi R. Manganese suppresses ATP-dependent intercellular calcium waves in astrocyte networks through alteration of mitochondrial and endoplasmic reticulum calcium dynamics. *Brain Res* 2006;1113:210–9. [PubMed: 16934782]
- [69]. Tong JJ, Schriener SE, McCleary D, Day BJ, Wallace DC. Life extension through neurofibromin mitochondrial regulation and antioxidant therapy for neurofibromatosis-1 in *Drosophila melanogaster*. *Nat Genet* 2007;39:476–85. [PubMed: 17369827]
- [70]. Trotter C, Serpell MG. Neurological sequelae in children after prolonged propofol infusion. *Anaesthesia* 1992;47:340–2. [PubMed: 1519689]
- [71]. Uhlen P. Spectral analysis of calcium oscillations. *Sci STKE* 2004;2004:p115. [PubMed: 15536176]
- [72]. Vajda FJ, Donnan GA, Phillips J, Bladin PF. Human brain, plasma, and cerebrospinal fluid concentration of sodium valproate after 72 hours of therapy. *Neurology* 1981;31:486–7. [PubMed: 6783980]
- [73]. Wysowski DK, Pollock ML. Reports of death with use of propofol (Diprivan) for nonprocedural (long-term) sedation and literature review. *Anesthesiology* 2006;105:1047–51. [PubMed: 17065900]
- [74]. Ya Deau JT, Morelli CM, Desravines S. Inhibition by propofol of intracellular calcium mobilization in cultured mouse pituitary cells. *Anesth Analg* 2003;97:1325–30. [PubMed: 14570647]
- [75]. Zhang S, Zhou Z, Fu J. Effect of manganese chloride exposure on liver and brain mitochondria function in rats. *Environ Res* 2003;93:149–57. [PubMed: 12963399]

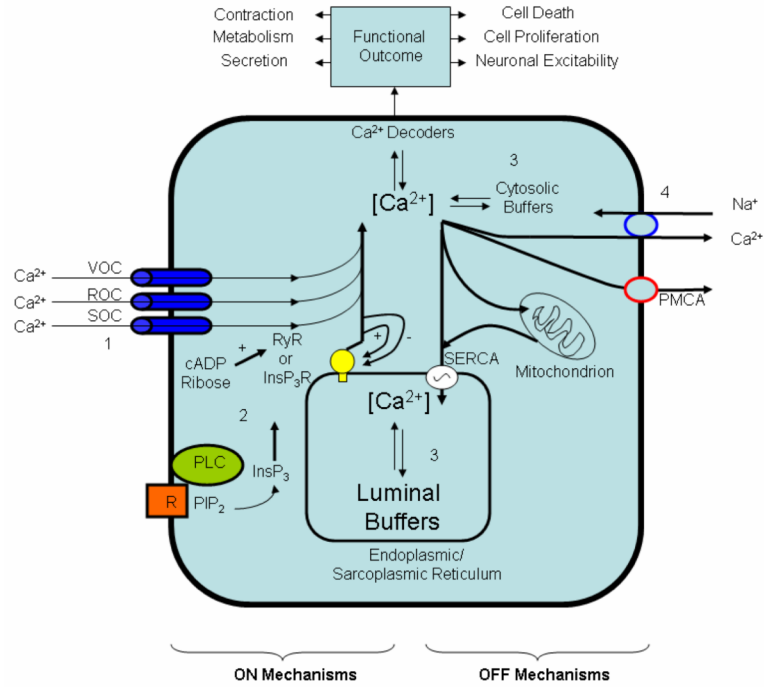


Figure 1.

ON and OFF mechanisms that regulate intracellular Ca^{2+} levels. The ON mechanisms involve the use of channels in the plasma membrane (voltage operated channels (VOC), receptor operated channels (ROC), store operated channels (SOC)) to allow entry of Ca^{2+} inside the cell or Ca^{2+} release through ryanodine receptors (RYRs) or inositol trisphosphate receptors (InsP3Rs). InsP3 mediated Ca^{2+} depletion of the ER activates store operated calcium entry necessary for the ER replenishment by translocating Orai1 molecules to the same locations of Stim1 molecules at close proximity of the plasma membrane [1]. The OFF mechanisms remove Ca^{2+} from the cytoplasm using cytosolic buffers (e.g, Ca^{2+} binding proteins) and pumps such as the membrane $\text{Na}^+/\text{Ca}^{2+}$ exchanger (found mainly in excitable cells) and the plasma membrane Ca^{2+} -ATPase (PMCA). PMCA is regulated by a variety of factors including calmodulin, acidic phospholipids, and protein kinases A and C (PKA and PKC). Mitochondria also play an important role in accumulating Ca^{2+} up to a level beyond which permeability transition pore develops that can lead to depolarization, release of cytochrome c and therefore apoptosis. This figure was adapted with permission from EMD BioSciences website where more detailed description of the ON and OFF mechanisms are outlined http://www.emdbiosciences.com/html/cbc/calcium_signaling.htm.

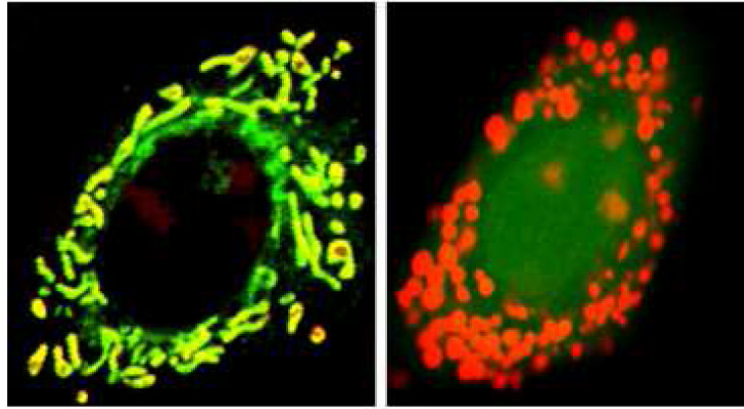


Figure 2.

An example of cells (right panel) loaded with fluo-4 and rhod2 to determine the ratio of mitochondrial to cytosolic Ca^{2+} used for steady state measurements. Note that rhod2 stains the mitochondrial calcium as well as the nucleoli. This was verified using cells loaded with rhod2 and mitotracker green (left panel).

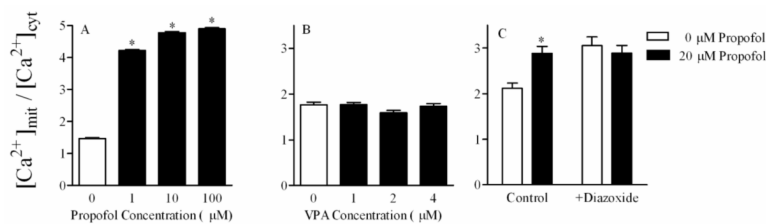


Figure 3.

Ratio of mitochondrial to cytosolic Ca^{2+} in CCF-STTG1 cells treated with different concentrations of propofol (A), or valproic acid (B). Data represent mean normalized fluorescence intensity \pm SE of at least 20 images per treatment. (C) Ratio of mitochondrial to cytosolic Ca^{2+} in CCF-STTG1 cells treated with 20 μM propofol for 72 h followed by 10 μM diazoxide for 1h prior to imaging and during loading of the fluorescent dyes rhod2 and fluo4. Asterisk indicates statistically significant changes from control values at $p < 0.05$. A portion of this data was adapted from reference [4] with permission.

$$Y = (A-B) * \exp(-K*t) + B$$

K = rate of wave propagation
Half life = $0.69/K$

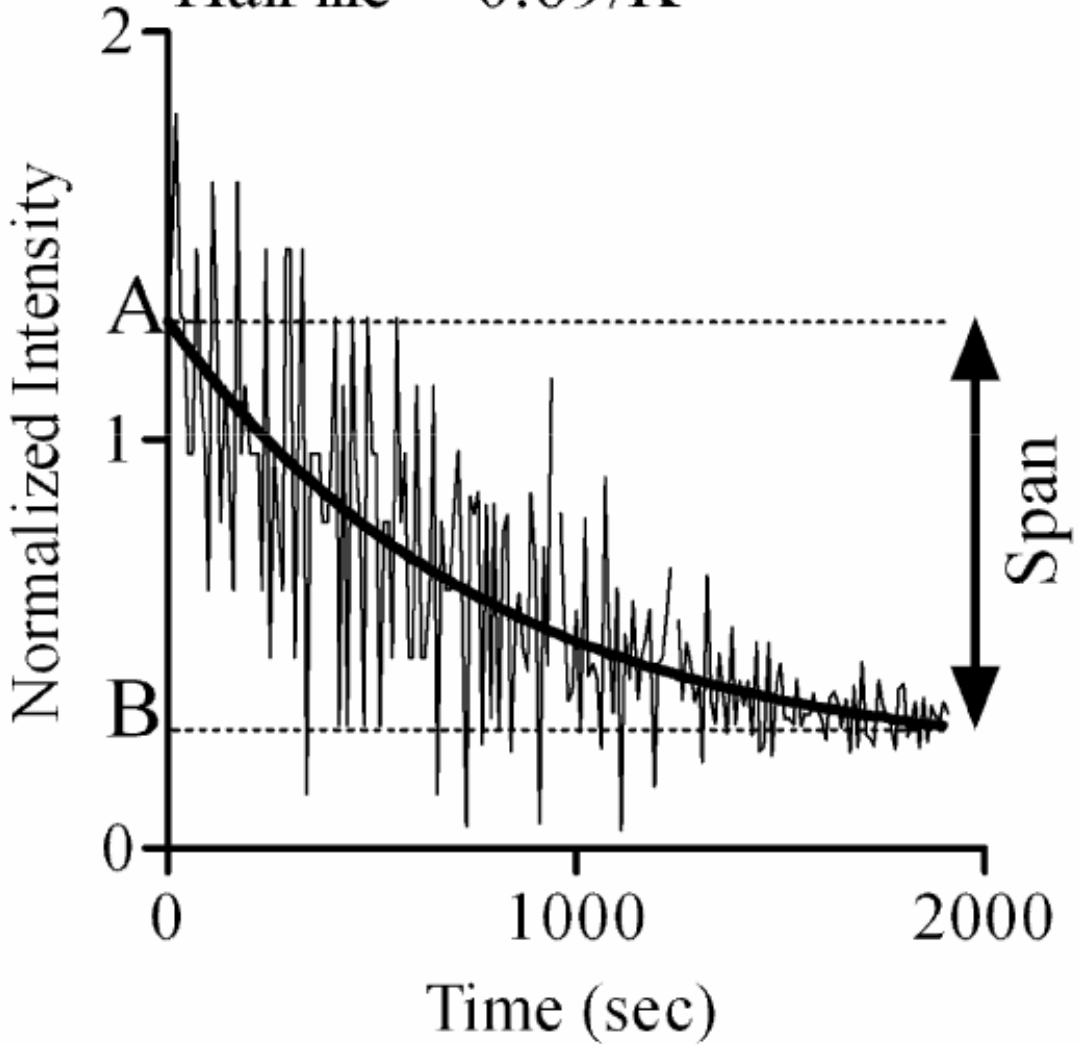


Figure 4. An example of Ca²⁺ wave initiated in CCF-STTG1 cells by addition of 10% FBS. The half-life and rate (K) of the wave were determined by fitting the experimental data to the non linear exponential equations described by Y. The noisy pattern observed in this response represents the oscillations detected in some cells in the imaged field. The Y-axis normalized intensity represents the ratio of fluo4 fluorescence intensity following FBS stimulation to basal fluo4 fluorescence intensity (before FBS stimulation). The decay in Ca²⁺ response is due to the wave disappearance. Please see the text for definitions of half-life, rate, and span.

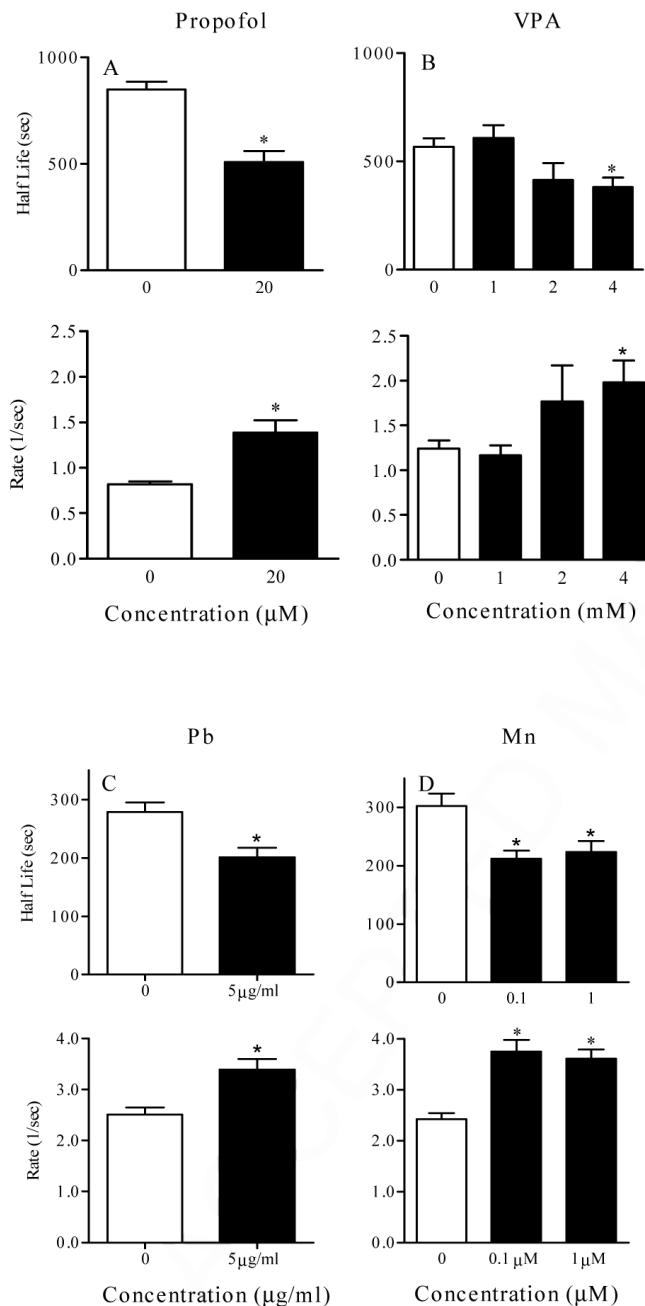


Figure 5.

Analysis of half-life and rate (K) of Ca^{2+} wave initiated in CCF-STTG1 cells treated for 24 hr with propofol (0, 20 μM) (top, left panel), valproic acid (0-4 mM) (top, right panel), lead (Pb) (0, 5 $\mu g/ml$) (bottom, left panel), and Manganese (Mn) (0- 1 μM) (bottom, right panel). In each experiment, cells were loaded with fluo4 for 1 h at 37° C and then washed with serum free medium. The wave was then generated by addition of 10% FBS and cells were imaged for approximately 30 min at 5 seconds interval. Data represented was collected from at least 8 images, 15 to 30 cells per image, per treatment. Asterisk represents significant difference from control at $p < 0.05$.

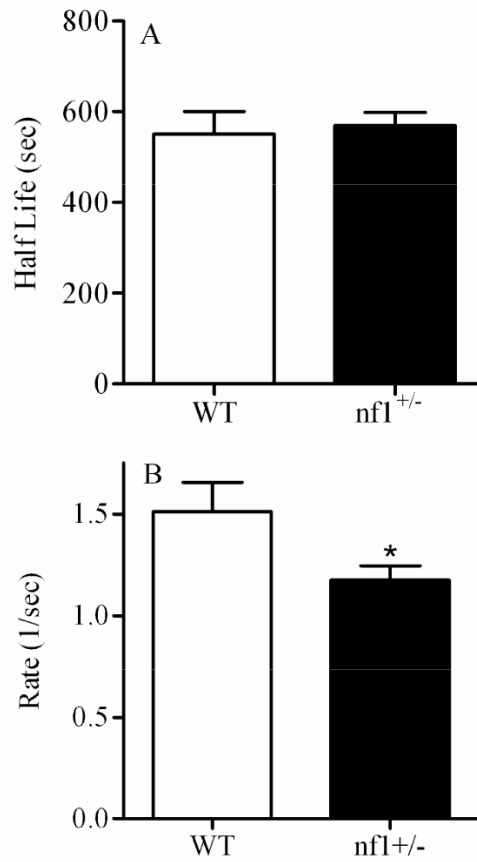


Figure 6. Analysis of Ca²⁺ wave initiated in wild type (WT) and *nfl*^{+/-} primary astrocytes using 10% FBS. Data represented was collected from at least 8 images, 15 to 30 cells per image, per treatment. Asterisk represents significant difference from control WT at p < 0.05.

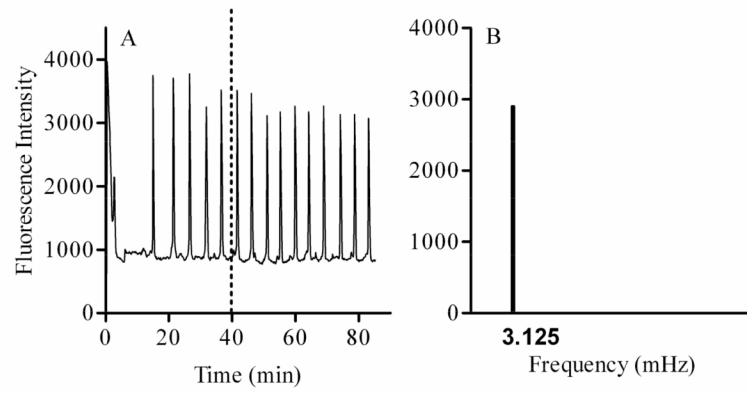


Figure 7.

An example of simple Ca^{2+} oscillations (A) initiated in myometrial cells following addition of 20 nM oxytocin. Fourier analysis of this data between 40 and 80min reveals the presence of one frequency of oscillation (B). Note that in case of a more complex signal, FFT will identify all the frequencies existing in the signal.

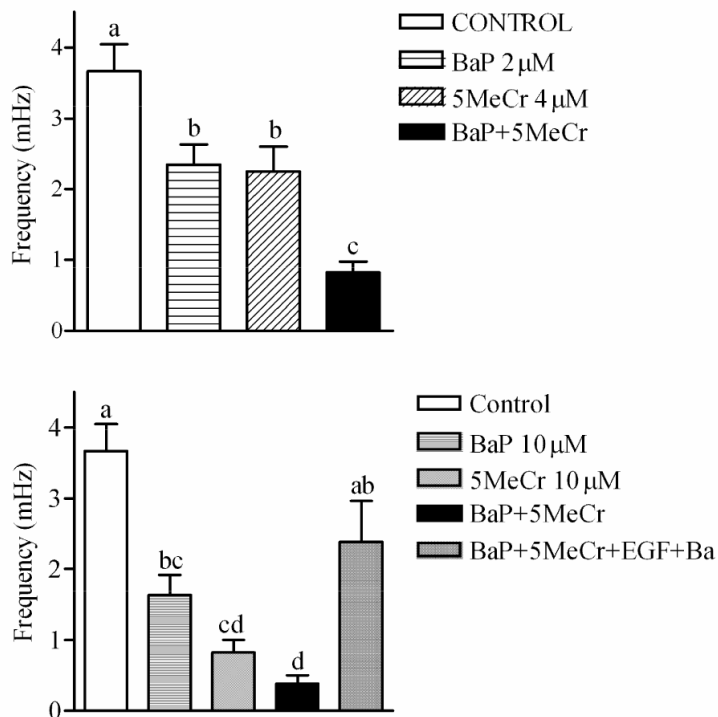


Figure 8.

Results from FFT in CCF-STTG1 cells stimulated with 10% FBS to induce oscillations following 24hrs treatment with: (A) 2 μ M BaP, 4 μ M 5-MeCr or a mixture of 2 μ M BaP and 4 μ M 5-MeCr and (B) 10 μ M BaP, 10 μ M 5-MeCr, or a mixture of 10 μ M BaP and 10 μ M 5-MeCr. Data represent at least 30 cells per treatment. Different letters indicate significant difference at $p < 0.05$ using Tukey's multiple comparison test. Note that EGF and Barium added 1hr prior to imaging and during loading of the Ca^{2+} probe fluo-4 were able to reverse the effects of the mixture of BaP and 5MeCr on the frequency of Ca^{2+} oscillations (B).